International Journal of Modern Physics A
Vol. 30, No. 24 (2015) 1550142 (9 pages)

DOI: 10.1142/S0217751X15501420

World Scientific
www.worldscientific.com

Combined fit to BESIII data on $e^+e^- \to h_c\pi^+\pi^-$ and $\chi_{c0}\omega$

X. N. Feng,*,† X. Y. Gao† and C. P. Shen†,‡

*School of Mathematics and System Science, Beihang University, Xueyuan Road No. 37, Haidian District, Beijing 100191, China
†School of Physics and Nuclear Energy Engineering, Beihang University, Xueyuan Road No. 37, Haidian District, Beijing 100191, China
‡shencp@ihep.ac.cn

Received 22 April 2015
Revised 15 June 2015
Accepted 2 July 2015
Published 6 August 2015

The cross-sections of $e^+e^- \to h_c\pi^+\pi^-$ and $\chi_{c0}\omega$ were measured by the BESIII experiment. In both cross-section distributions, there are structures at a mass of about 4220 MeV/c^2. A combined fit is performed to the two cross-section distributions, assuming the structures are due to the same vector resonant state, the $Y(4220)$. The parameters of the $Y(4220)$ are determined using two fit methods. The ratios $\Gamma(Y(4220) \to \chi_{c0}\omega)/\Gamma(Y(4220) \to h_c\pi^+\pi^-)$ are obtained, which may help in the understanding of the nature of this structure. Although a similar work was done previously, all the multiple solutions in our fits are taken into account and our conclusions are more precise and complete.

Keywords: Combined fit; the $Y(4220)$; multiple solutions; tetraquark.

PACS numbers: 02.60.Cb, 13.66.Bc, 14.40.Rt, 14.40.Pq

1. Introduction

During the last decade, many new charmonium-like states were discovered, such as the $X(3872)$,[1] the $Y(4260)$[2,3] and the $Z_c(3900)$.[3,4] They cannot be identified as conventional $c\bar{c}$ states (for a review see for example, Refs. 5 and 6). Among these new charmonium-like states, there are many vector states ($J^{PC} = 1^{--}$) above $D\bar{D}$ threshold that are usually called Y-states, like the $Y(4260)$,[2,3] the $Y(4360)$,[7–9] and the $Y(4660)$.[8,10] According to the potential models, there should be only five vector states above the well-known $1D$ state $\psi(3770)$ and below about 4.7 GeV/c^2. They are $3S$, $2D$, $4S$, $3D$ and $5S$ states.[11] However, experimentally more Y-states

‡Corresponding author.

besides the well-established $\psi(4040)$, $\psi(4160)$ and $\psi(4415)$[12] have been found. These states provide strong evidence for the existence of exotic QCD states and stimulate many theoretical explanations such as tetraquarks, molecules, hybrids, hadrocharmonia.[5,6]

In recent years, BESIII, running above open charm threshold, has obtained many results that may help in the understanding of the nature of these charmonium-like states. The most prominent ones are the observations of the charged charmonium-like states, the $Z_c(3900)$ and $Z_c(4020)$, observed in $e^+e^- \to J/\psi\pi^+\pi^-$ [4] and $h_c\pi^+\pi^-$,[13] respectively. In $e^+e^- \to h_c\pi^+\pi^-$, besides the observation of the $Z_c(4020)$, BESIII also reported cross-section measurements at 13 center-of-mass (CM) energy points from 3.900 GeV to 4.420 GeV.[13] The measured $e^+e^- \to h_c\pi^+\pi^-$ cross-sections are shown in Fig. 1(a), where the error bars are statistical uncertainties only. The systematic error (9%) is common for all data points. From the cross-section distribution, there is a very interesting structure at around 4.22 GeV/c^2.

The BESIII experiment also recently reported the cross-section measurements of $e^+e^- \to \chi_{c0}\omega$ at 9 CM energies from 4.21 to 4.42 GeV. Figure 1(b) shows the measured Born cross-sections, where the uncertainties are statistical only.[14] The systematic errors, ranging from 6.7% to 16.1% depending on CM energy, are not included since they are small compared to the statistical errors.

BESIII found that the distribution had a structure around 4.22 GeV/c^2 and was inconsistent with the line shape of the $Y(4260)$ observed in $e^+e^- \to \pi^+\pi^- J/\psi$. Assuming the observed $\chi_{c0}\omega$ structure comes from a single resonance, the measured mass and width are $(4230 \pm 8 \pm 6)$ MeV/c^2 and $(38 \pm 12 \pm 2)$ MeV, respectively, and the statistical significance is more than 9σ.[14] After the $e^+e^- \to \chi_{c0}\omega$ cross-section results were published, a few theoretical models were proposed to interpret the newly observed structure at 4.23 GeV/c^2: a tetraquark state;[15] the missing higher charmonium state $\psi(4S)$;[16] and the known charmonium-like resonance $\psi(4160)$ with the mass of about 4190 MeV/c^2.[17]

Since the resonance parameters including peak position and width of the two channels $h_c\pi^+\pi^-$ and $\chi_{c0}\omega$ are very similar, in this paper we do a combined fit to the BESIII $e^+e^- \to h_c\pi^+\pi^-$ and $\chi_{c0}\omega$ cross-section distributions assuming the observed two peaks at about 4.22 GeV are from the same resonance, named $Y(4220)$ hereafter.

We fit the cross-sections with two different models (I and II in the following): the coherent sum of two amplitudes, a constant and a constant width relativistic Breit–Wigner (BW) function (model I); and the coherent sum of two constant width relativistic BW functions for $h_c\pi^+\pi^-$ and the coherent sum of a constant and a constant width relativistic BW function for $\chi_{c0}\omega$ (model II). Since the interference is included in the fits, multi-solution problem will be discussed in Sec. 2. A brief discussion of available fit results is given in Sec. 3. In addition,

our fit results will be shown in detail. Finally, a discussion and summary are given in Sec. 4.

2. Multiple Solution Problem

Interference is a natural and common phenomenon in the world. In classical physics, if two waves meet, what we see is the sum of the two amplitudes. In quantum mechanics, what we observe is the total amplitude, too. When it comes to interference, the final results may come from two possibilities: constructive interference or destructive interference.

Taking two BWs with interference as an example in the fit, we face the multi-solution problem with two prominent characteristics: (1) all sets of solutions have equal goodness-of-fit; (2) the masses and the total widths are the same, but the partial widths and the relative phase between the amplitudes are different. Therefore with the interference included in the fitting process, we need to make sure that all multiple solutions are found although sometimes some solutions are very close or exactly the same. Experimental results may not be complete or even be biased if only one solution is reported while there are twofold amplitudes. If one solution has already been found by fitting, the other solution can even be derived via mathematical calculation.[18] It allows us to do a cross-check to make sure no solution is missed.

3. Our Fit Results

In order to obtain the $Y(4220)$ resonance parameters, we do a combined fit to the $h_c\pi^+\pi^-$ and $\chi_{c0}\omega$ cross section distributions using a least squares method with MINUIT in the CERN Program Library.[19] We will fit the data with two different scenarios.

For model I, we fit both the $h_c\pi^+\pi^-$ and $\chi_{c0}\omega$ cross sections with the coherent sum of a BW and a pure phase-space background. The mass and width of the $Y(4220)$ are constrained to be the same in both channels. The fitting functions are:

$$\sigma_{h_c\pi^+\pi^-}(m) = \left| A + \frac{Be^{i\phi_1}}{\sqrt{PS_3(M)}}\,\mathrm{BW}(m, M, \Gamma) \right|^2 PS_3(m)\,, \tag{1}$$

$$\sigma_{\chi_{c0}\omega}(m) = \left| C + \frac{De^{i\phi_2}}{\sqrt{PS_2(M)}}\,\mathrm{BW}(m, M, \Gamma) \right|^2 PS_2(m)\,, \tag{2}$$

where M and Γ are the mass and width of the $Y(4220)$, m is the invariant mass of the system, $\mathrm{BW}(m, M, \Gamma) = (m^2 - M^2 + iM\Gamma)^{-1}$, $B = \sqrt{12\pi\mathcal{B}_{h_c\pi^+\pi^-}\Gamma_{e^+e^-}\Gamma}$, $D = \sqrt{12\pi\mathcal{B}_{\chi_{c0}\omega}\Gamma_{e^+e^-}\Gamma}$ and PS_n is the n-body phase-space.

For model II, we fit the $h_c\pi^+\pi^-$ cross-sections with the coherent sum of two constant width relativistic BW functions; that is the background is parametrized

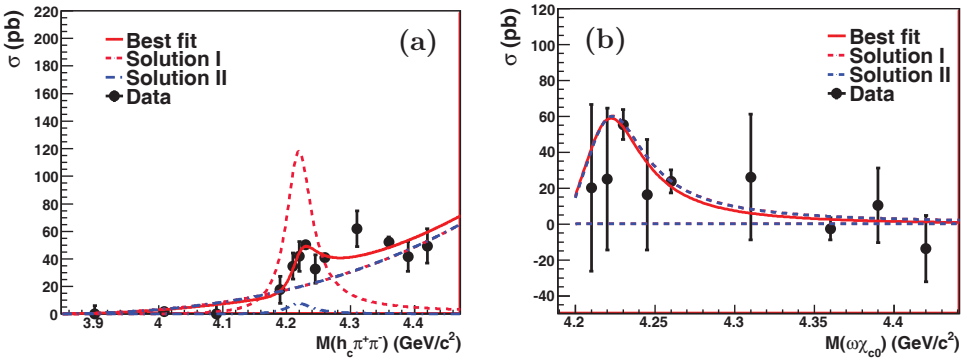

Fig. 1. The results of the fit to $e^+e^- \to h_c\pi^+\pi^-$ and $\chi_{c0}\omega$ data from BESIII with the fitting functions defined in model I. The curves show the projections from the best fit. The interference between the two amplitudes is not shown. For $h_c\pi^+\pi^-$, the two dashed curves show the two solutions (see Table 1), one is for the destructive solution (Solution I), the other is for the constructive solution (Solution II). For $\chi_{c0}\omega$, the differences between the two solutions are not visible.

by a broad BW. The fitting functions are:

$$\sigma_{h_c\pi^+\pi^-}(m) = \left| \frac{B_1}{\sqrt{PS_3(M_1)}} \mathrm{BW}_1(m, M_1, \Gamma_1) + \frac{B_2 e^{i\phi_1}}{\sqrt{PS_3(M_2)}} \mathrm{BW}_2(m, M_2, \Gamma_2) \right|^2 PS_3(m)\,, \tag{3}$$

$$\sigma_{\chi_{c0}\omega}(m) = \left| C + \frac{D e^{i\phi_2}}{\sqrt{PS_2(M_1)}} \mathrm{BW}(m, M_1, \Gamma_1) \right|^2 PS_2(m)\,. \tag{4}$$

Figure 1 shows the fit results using the functions defined in model I, with a goodness-of-the-fit of $\chi^2/\mathrm{ndf} = 12.2/15$, corresponding to a confidence level (C.L.) of 66.4%. The two solutions for the $\chi_{c0}\omega$ corresponding to the same solution in $h_c\pi^+\pi^-$ are almost the same, so there are in total two groups of solutions with equally good fit quality. The masses and the widths of the $Y(4220)$ in the two solutions are identical but the products of the branching fraction and partial width to e^+e^- and relative phases are different, as shown in Table 1. The correlations between the fit parameters are shown in Table 2. The resonance parameters of the $Y(4220)$ are $M = (4218 \pm 7)$ MeV/c^2 and $\Gamma = (48 \pm 10)$ MeV. The errors are statistical from the fit only. As a validation and a cross-check, we take a solution, for example "Solution I", as input and calculate the other solution mathematically.[18] The other solution is the same as that of "Solution II" from the fit.

We also perform a combined fit with the functions defined in model II. The result is shown in Fig. 2. There are two solutions, and the results for these two solutions with a goodness-of-the-fit of $\chi^2/\mathrm{ndf} = 5.1/13$, corresponding to a C.L. of 97.3%, are shown in Table 3. The correlations between the fit parameters are shown in Table 4. The fitted values of the mass and width of the $Y(4220)$ are

Table 1. Fit results to the combined BESIII data on $e^+e^- \to h_c\pi^+\pi^-$ and $\chi_{c0}\omega$ with the functions defined in model I. The errors are only statistical from the fit. M, Γ and $\mathcal{B}_i \times \Gamma_{e^+e^-}$ ($i = h_c\pi^+\pi^-$, $\chi_{c0}\omega$) are the mass (in MeV/c^2), total width (in MeV) and product of the branching fraction to $h_c\pi^+\pi^-/\chi_{c0}\omega$ and the e^+e^- partial width (in eV/c^2), respectively. ϕ is the relative phase (in rad).

	Solution I	Solution II
$M(Y(4220))$	4218 ± 7	
$\Gamma(Y(4220))$	48 ± 10	
$\mathcal{B}_{h_c\pi^+\pi^-} \times \Gamma_{e^+e^-}$	6.9 ± 1.4	0.5 ± 0.2
ϕ_1	4.9 ± 0.2	0.7 ± 0.4
$\mathcal{B}_{\chi_{c0}\omega} \times \Gamma_{e^+e^-}$	3.3 ± 1.2	3.3 ± 0.8
ϕ_2	0.1 ± 3.1	0.1 ± 1.9
χ^2/ndf	12.2/15	

Table 2. The correlations between the fit parameters shown in Table 1 (with the units given there). The numbers in parentheses are for the second solution.

	$\Gamma(Y(4220))$	$\mathcal{B}_{h_c\pi^+\pi^-} \times \Gamma_{e^+e^-}$	ϕ_1	$\mathcal{B}_{\chi_{c0}\omega} \times \Gamma_{e^+e^-}$	ϕ_2
$M(Y(4220))$	−0.38 (−0.40)	0.40 (−0.85)	−0.85 (0.83)	−0.34 (−0.57)	−0.01 (−0.05)
$\Gamma(Y(4220))$	1.00	0.62 (0.55)	0.16 (−0.11)	0.65 (0.90)	0.16 (0.13)
$\mathcal{B}_{h_c\pi^+\pi^-} \times \Gamma_{e^+e^-}$	0.62 (0.55)	1.00	−0.67 (−0.82)	0.33 (0.71)	0.13 (0.16)
ϕ_1	0.16 (−0.11)	−0.67 (−0.82)	1.00	0.20 (−0.38)	0.01 (−0.10)
$\mathcal{B}_{\chi_{c0}\omega} \times \Gamma_{e^+e^-}$	0.65 (0.90)	0.33 (0.71)	0.20 (−0.38)	1.00	0.72 (0.37)

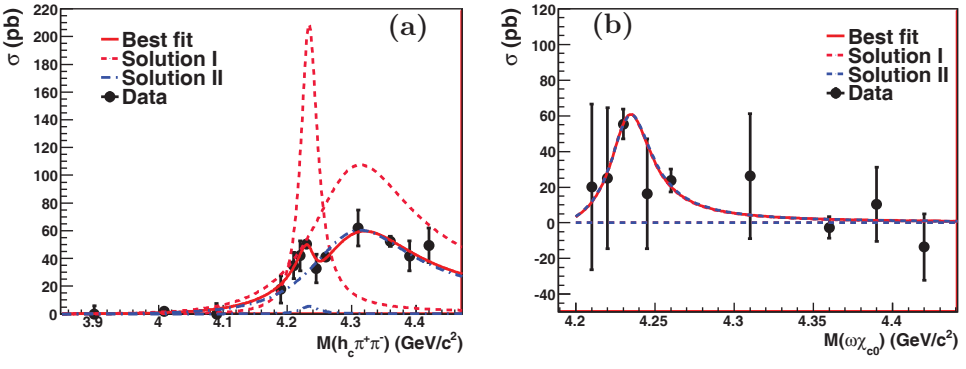

Fig. 2. The results of the combined fit to $e^+e^- \to h_c\pi^+\pi^-$ and $\chi_{c0}\omega$ data with the fitting functions defined in model II. The curves show the projections from the best fit. For $h_c\pi^+\pi^-$, the two dashed curves show the two solutions (see Table 3), one is for the destructive solution (Solution I), and the other is for the constructive solution (Solution II). For $\chi_{c0}\omega$, the differences between the two solutions are not visible.

Table 3. Fit results to the BESIII $e^+e^- \to h_c\pi^+\pi^-$ and $\chi_{c0}\omega$ cross-section distributions with the functions defined in model II. The errors are statistical from fit only. M_j, Γ_j and $(\mathcal{B}_i \times \Gamma_{e^+e^-})_j$ ($i = h_c\pi^+\pi^-$, $\chi_{c0}\omega$) are the mass (in MeV/c^2), total width (in MeV), and product of the branching fraction to $h_c\pi^+\pi^-/\chi_{c0}\omega$ and the e^+e^- partial width (in eV/c^2), respectively, where $j = 1$ for the $Y(4220)$ and $j = 2$ for the background parametrization. ϕ is the relative phase (in rad).

	Solution I	Solution II
$M_1(Y(4220))$	4233 ± 3	
$\Gamma_1(Y(4220))$	32 ± 12	
$(\mathcal{B}_{h_c\pi^+\pi^-} \times \Gamma_{e^+e^-})_1$	8.5 ± 1.0	0.2 ± 0.2
ϕ_1	3.7 ± 0.1	-0.6 ± 0.5
M_2	4290 ± 10	
Γ_2	192 ± 36	
$(\mathcal{B}_{h_c\pi^+\pi^-} \times \Gamma_{e^+e^-})_2$	25.1 ± 2.2	13.7 ± 2.0
$\mathcal{B}_{\chi_{c0}\omega} \times \Gamma_{ee}$	2.3 ± 0.7	2.4 ± 0.5
ϕ_2	-2.1 ± 2.1	-0.3 ± 1.1
χ^2/ndf	5.1/13	

Table 4. The correlations between the fit parameters shown in Table 3 (with the units given there). The numbers in parentheses are for the second solution.

	$\Gamma_1(Y(4220))$	$(\mathcal{B}_{h_c\pi^+\pi^-} \times \Gamma_{e^+e^-})_1$	ϕ_1	M_2
$M_1(Y(4220))$	-0.12 (-0.65)	0.05 (-0.90)	-0.25 (-0.55)	-0.34 (-0.59)
$\Gamma_1(Y(4220))$	1.00	0.96 (0.86)	-0.26 (0.77)	-0.01 (0.68)
$(\mathcal{B}_{h_c\pi^+\pi^-} \times \Gamma_{e^+e^-})_1$	0.96 (0.86)	1.00	-0.30 (0.79)	-0.25 (0.80)
ϕ_1	-0.26 (0.77)	-0.30 (0.79)	1.00	0.44 (0.94)
M_2	-0.01 (0.68)	-0.25 (0.80)	0.44 (0.94)	1.00
Γ_2	0.15 (-0.15)	0.08 (-0.54)	-0.88 (-0.49)	-0.07 (-0.60)
$(\mathcal{B}_{h_c\pi^+\pi^-} \times \Gamma_{e^+e^-})_2$	0.88 (-0.61)	0.94 (-0.80)	-0.52 (-0.87)	-0.36 (-0.83)
$\mathcal{B}_{\chi_{c0}\omega} \times \Gamma_{ee}$	0.71 (0.87)	0.75 (0.65)	-0.31 (0.68)	-0.13 (0.57)
	Γ_2	$(\mathcal{B}_{h_c\pi^+\pi^-} \times \Gamma_{e^+e^-})_2$	$\mathcal{B}_{\chi_{c0}\omega} \times \Gamma_{ee}$	ϕ_2
$M_1(Y(4220))$	-0.03 (0.64)	0.12 (0.70)	0.40 (-0.40)	-0.34 (0.54)
$\Gamma_1(Y(4220))$	0.15 (-0.15)	0.88 (-0.61)	0.71 (0.87)	-0.28 (-0.37)
$(\mathcal{B}_{h_c\pi^+\pi^-} \times \Gamma_{e^+e^-})_1$	0.08 (-0.54)	0.94 (-0.80)	0.75 (0.65)	-0.32 (-0.52)
ϕ_1	-0.88 (-0.49)	-0.52 (-0.87)	-0.31 (0.68)	0.17 (-0.38)
M_2	-0.07 (-0.60)	-0.36 (-0.83)	-0.13 (0.57)	0.11 (-0.40)
Γ_2	1.00	0.32 (0.79)	0.10 (0.01)	-0.04 (0.38)
$(\mathcal{B}_{h_c\pi^+\pi^-} \times \Gamma_{e^+e^-})_2$	0.32 (0.79)	1.00	0.72 (-0.47)	-0.32 (0.44)
$\mathcal{B}_{\chi_{c0}\omega} \times \Gamma_{ee}$	0.10 (0.01)	0.72 (-0.47)	1.00	-0.78 (-0.3)

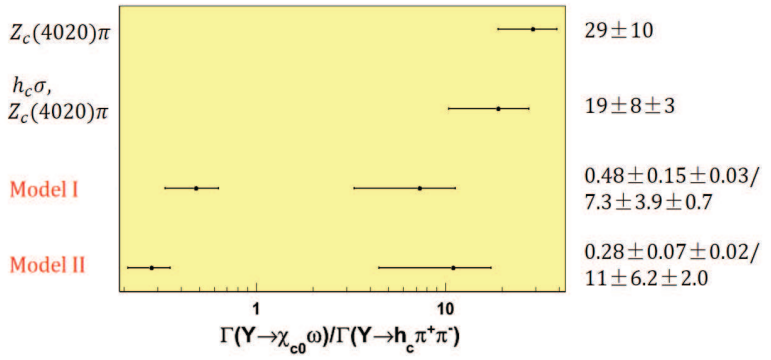

Fig. 3. The distribution of the measured ratios of $\Gamma(Y(4220) \to \chi_{c0}\omega)/\Gamma(Y(4220) \to h_c\pi^+\pi^-)$ together with the theoretical predictions with the assumption that the $Y(4220)$ is a tetraquark state. The error bars are the total errors of the statistical and systematic uncertainties added in quadrature.

$M = (4233 \pm 3)$ MeV/c^2 and $\Gamma = (32 \pm 12)$ MeV, where the errors are statistical only. They are consistent with the above results within 2σ.

By comparing the BW amplitudes in the $h_c\pi^+\pi^-$ and $\chi_{c0}\omega$ channels from the $Y(4220)$ decays, we obtain ratios $\Gamma(Y(4220) \to \chi_{c0}\omega)/\Gamma(Y(4220) \to h_c\pi^+\pi^-)$,[a] which are $0.48 \pm 0.15 \pm 0.03$ for destructive solution and $7.3 \pm 3.9 \pm 0.7$ for the construction solution in model I; $0.28 \pm 0.07 \pm 0.02$ for destructive solution and $11 \pm 6.2 \pm 2.0$ for the construction solution in model II. Here, the first uncertainty is only the statistical error from fit and the second one is the sum of the systematic errors in the $h_c\pi^+\pi^-$ [13] and $\chi_{c0}\omega$ [14] cross-section measurements added in quadrature. Figure 3 shows the distribution of the measured ratios of $\Gamma(Y(4220) \to \chi_{c0}\omega)/\Gamma(Y(4220) \to h_c\pi^+\pi^-)$ together with the theoretical predictions assuming the $Y(4220)$ is a tetraquark state and the decay $Y(4220) \to h_c\pi^+\pi^-$ is dominated by the intermediate processes $Z_c(4020)^\pm\pi^\mp$ or $Z_c(4020)^\pm\pi^\mp$ plus $h_c\sigma$.[15]

4. Discussion and Summary

In this paper, we do combined fits to the $e^+e^- \to h_c\pi^+\pi^-$ and $\chi_{c0}\omega$ cross-sections measured by BESIII with two different scenarios assuming the observed structures at about 4.22 GeV/c^2 are from the same $Y(4220)$ resonance decays. In these two different scenarios, two amplitudes with interference are used. In the fits to $h_c\pi^+\pi^-$, two different solutions corresponding to constructive and destructive interferences, respectively, are found, while for the $\chi_{c0}\omega$, the two solutions are almost the same. The mass, width and product branching fraction to $h_c\pi^+\pi^-/\chi_{c0}\omega$

[a]The ratio is obtained from the fit as a free parameter instead of the calculation using the values of $\mathcal{B}_{\chi_{c0}\omega} \times \Gamma_{e^+e^-}$ and $\mathcal{B}_{h_c\pi^+\pi^-} \times \Gamma_{e^+e^-}$ directly to make the correlation error between the two channels considered automatically and correctly. As a cross check, the central value of the ratio from the fit as a free parameter is the same as the ratio of $\mathcal{B}_{\chi_{c0}\omega} \times \Gamma_{e^+e^-}$ and $\mathcal{B}_{h_c\pi^+\pi^-} \times \Gamma_{e^+e^-}$.

and the e^+e^- partial width are determined for the $Y(4220)$ in each fit. All the fit results are summarized in Tables 1 and 3. In addition, the measured ratios $\Gamma(Y(4220) \to \chi_{c0}\omega)/\Gamma(Y(4220) \to h_c\pi^+\pi^-)$ corresponding to constructive and destructive interferences are obtained. The ratios from constructive fits are consistent with the theoretical predictions under the assumption of the $Y(4220)$ being a tetraquark state within 2σ, while the ones from destructive fits are not. So we cannot conclude that the $Y(4220)$ must be a tetraquark state since we do not know which solution is the real physical one.

The possible structure in the $e^+e^- \to h_c\pi^+\pi^-$ cross-section distribution was noted by the authors in Refs. 15 and 20. The author in Ref. 20 did fits to the $e^+e^- \to h_c\pi^+\pi^-$ cross-sections since no measurements were available for $\chi_{c0}\omega$ at that time. Although the authors in Ref. 15 did combined fits to the $e^+e^- \to h_c\pi^+\pi^-$ and $\chi_{c0}\omega$ cross-sections with the same two fitting scenarios as described in this text, only constructive solutions were found. Based on the ratio from the constructive solutions, they concluded that the structures seen in $h_c\pi^+\pi^-$ and $\chi_{c0}\omega$ can be explained within the diquark–antidiquark model. With only one solution, the conclusion is questionable.

Here, we also would like to point out more measurements from the BESIII experiment at CM energies above 4.42 GeV and more precise data at around the $Y(4220)$ peak are crucial to make sure the structure is a real resonance. Especially for $h_c\pi^+\pi^-$, more measurements at masses higher than 4.5 GeV are needed to discriminate experimentally between the two models. Considering the maximum energy point that BESIII experiment can reach is 4.6 GeV, the BelleII experiment is more promising in the future, where the processes $e^+e^- \to h_c\pi^+\pi^-$ and $\chi_{c0}\omega$ can be investigated via initial state radiation with large data sample.

Acknowledgments

We would like to thank Professor Frederick A. Harris for useful comments and revise in the text. We acknowledge support in part by the Fundamental Research Funds for the Central Universities YWF-14-WLXY-013, National Key Basic Research Program of China under Contract No. 2015CB856701 and CAS Center for Excellence in Particle Physics (China).

Note Added

After we submitted this paper, we became aware of the revised version of Ref. 15, where the authors found the two solutions based on our reminder.

References

1. Belle Collab. (S. K. Choi *et al.*), *Phys. Rev. Lett.* **91**, 262001 (2003), arXiv:hep-ex/0309032.
2. BaBar Collab. (B. Aubert *et al.*), *Phys. Rev. D* **86**, 051102 (2012), arXiv:1204.2158.
3. Belle Collab. (Z. Q. Liu *et al.*), *Phys. Rev. Lett.* **110**, 252002 (2013), arXiv:1304.0121.

4. BESIII Collab. (M. Ablikim *et al.*), *Phys. Rev. Lett.* **110**, 252001 (2013), arXiv:1303.5949.
5. N. Brambilla *et al.*, *Eur. Phys. J. C* **74**, 2981 (2014), arXiv:1404.3723.
6. A. Esposito, A. L. Guerrieri, F. Piccinini, A. Pilloni and A. D. Polosa, *Int. J. Mod. Phys. A* **30**, 1530002 (2015), arXiv:1411.5997.
7. BaBar Collab. (B. Aubert *et al.*), *Phys. Rev. Lett.* **98**, 212001 (2007), arXiv:hep-ex/0610057.
8. Belle Collab. (X. L. Wang *et al.*), *Phys. Rev. Lett.* **99**, 142002 (2007), arXiv:0707.3699.
9. BaBar Collab. (B. Aubert *et al.*), *Phys. Rev. D* **89**, 111103 (2014), arXiv:1211.6271.
10. Belle Collab. (X. L. Wang *et al.*), *Phys. Rev. D* **91**, 112007 (2015), arXiv:1410.7641.
11. N. Brambilla *et al.*, *Eur. Phys. J. C* **71**, 1534 (2011), arXiv:1010.5827.
12. Particle Data Group (K. A. Olive *et al.*), *Chin. Phys. C* **38**, 090001 (2014).
13. BESIII Collab. (M. Ablikim *et al.*), *Phys. Rev. Lett.* **111**, 242001 (2013), arXiv:1309.1896.
14. BESIII Collab. (M. Ablikim *et al.*), *Phys. Rev. Lett.* **114**, 092003 (2015), arXiv:1410.6538.
15. R. Faccini, G. Filaci, A. Guerrieri, A. Pilloni and A. Polosa, arXiv:1412.7196v1.
16. D.-Y. Chen, X. Liu and T. Matsuki, *Phys. Rev. D* **91**, 094023 (2015), arXiv:1411.5136.
17. X. Li and M. B. Voloshin, *Phys. Rev. D* **91**, 034004 (2015), arXiv:1411.2952.
18. K. Zhu, X. Mo, C. Yuan and P. Wang, *Int. J. Mod. Phys. A* **26**, 4511 (2011), arXiv:1108.2760.
19. J. James, MINUIT, CERN Program Library Writeup Report No. D506.
20. C. Z. Yuan, *Chin. Phys. C* **38**, 043001 (2014), arXiv:1312.6399.